# Ground Speed Measuring System for Autonomous Vehicles

Yasmine Sheila Antille, Etienne Gubler and Juan-Mario Gruber
*Institute of Embedded Systems, Zurich University of Applied Sciences, Winterthur, Switzerland*

Keywords: Sensor Fusion, Ground Speed, Autonomous Driving, Driverless, Inertial Measurement Unit, Global Positioning System, Kalman Filter.

Abstract: In this paper a Ground Speed Measuring System which can measure the ground speed over the ground in three dimensions is proposed. The system uses two Kalman filters to compute the final ground speed based on the readings from its various sensors. The proposed solution combines state of the art techniques from different fields of sensor technology and will be incorporated into the high-performance driverless vehicle after completion of this project. The findings and learnings of developing this system are discussed and an evaluation of the module is presented. In the end, the system can accurately estimate a test vehicle's ground speed during system field tests.

## 1 INTRODUCTION

To be able to drive autonomously, a car depends on precise sensor data and accurate algorithmic calculations. Lots of various kinds of information is required for autonomous driving. One of them is the speed of movement of the vehicle over the ground. To determine the ground speed of an autonomously driving vehicle, multiple sensors can be fused together to form a fail-safe system.

In this body of work we evaluate some of the different possible approaches and then propose the design and construction of a ground speed sensor that measures the speed over the ground in 3 dimensions, and which can pass the data on to the control unit of the vehicle. A prototype, focused on economic efficiency, is developed and introduced and the implementation is discussed. The algorithms and system architecture are presented, which are designed for robustness, reliability, and extensibility. The ground speed measuring system is designed to accurately measure and uses a set of measurements generated by different sensors. The readings from these sensors must be combined to determine an estimate of the ground speed that is as accurate as possible.

This work is carried out in cooperation with the Formula Student ZHAW team and in close contact with the driverless and electrical engineering teams.

## 2 GROUND SPEED SENSOR FOR AUTONOMOUS VEHICLES

Driverless vehicles are autonomous cars in which human drivers are never required to take control to safely operate the vehicles. They combine sensors and software to control, navigate, and drive the vehicle without any human influence.

With a ground speed sensor and a suitable sensor fusion algorithm, the vehicle's odometry data will be much more accurate than without such a system. Having an accurate ground speed measurement can therefore help refine the vehicle's position while mapping an environment. In addition, this will allow for longer periods between the corrections the mapping algorithm has to undertake. With a Ground Speed Measuring System (GSMS), it will also be possible to recognize if one or more wheels lose traction on the ground which could lead to an unfortunate situation known as understeering. Like humans, autonomous vehicles could have difficulties adapting quickly to loss of traction, therefore recognizing such a situation as soon as possible can make a huge difference in reaction time.

### 2.1 Formula Student

Formula Student is a worldwide competitive design competition for student teams with the aim of building a race car. It provides a platform to student



Antille, Y., Gubler, E. and Gruber, J.
Ground Speed Measuring System for Autonomous Vehicles.
DOI: 10.5220/0010543106610668
In *Proceedings of the 18th International Conference on Informatics in Control, Automation and Robotics (ICINCO 2021)*, pages 661-668
ISBN: 978-989-758-522-7

engineering teams for developing and enhancing vehicle technologies in multiple domains. There are three different competition categories: combustion engine vehicles, electric vehicles and driverless vehicles. The driverless category is the most recently added one, having started in 2017. In the Formula Student Driverless competition, a team is tasked to build an autonomous race car that can complete the racetracks without a driver's influence by only using onboard sensors and computers. The Formula Student ZHAW team was formed by students from different engineering backgrounds at the Zurich University of Applied Sciences with the intention of competing in the electric and driverless categories.

## 2.2 Related Work

Since 2017, hundreds of Formula Student teams have been working on driverless vehicles. Outstanding results and various publications have been delivered by the Academic Motorsports Club Zurich (AMZ) from ETH Zurich.

In 2019, the AMZ-Racing driverless team published a comprehensive report on the concept of their first driverless racing car for the 2017/2018 racing season (Kabzan et al., 2017). The software-hardware architecture of the developed *"gotthard"* system is designed as follows. The software stack is divided in three main modules: Perception, Motion Estimation and Mapping and Control. Following the architecture design, the velocity estimation is used to compensate the motion distortion in the Lidar pipeline, propagate the state in the SLAM (Simultaneous Localization and Mapping) algorithm, as well as input for the control module. AMZ states in the report that the velocity estimation needs to combine data from various sensors with a vehicle model in order for it to be robust against sensor failure and to compensate for model mismatch and sensor inaccuracies. AMZ proposes to use a nine state Extended Kalman Filter (EKF), which fuses data from six different sensors.

AMZ also present the state estimation and system integration for an autonomous race car in and testify that sensor faults are a major factor undermining the robustness of state estimation systems and, therefore, a probabilistic outlier detection method should be used that works with any sensor. Their approach makes use of the innovation covariance calculated in the EKF which intrinsically accounts for the uncertainty of the state and the sensor noise model. Furthermore, they determine that if wheel odometry is the only velocity source, and if the wheels are constantly blocked due to high accelerations, the velocity estimate deteriorates (Valls et al., 2018).

Of course, AMZ is not the only Formula Student team that has achieved great results with a self-developed measuring system that subsequently results in a ground speed estimation. To name a couple of other remarkable approaches, two teams solved this problem in the following ways:

The Viennese TUW Racing team uses a differential Global Positioning System (GPS), provided by a Piksi Multi GNSS module along with two beacons placed outside the racetrack. The beacons allow for more precise positioning than a generic GPS system does. To measure the relative movement of the vehicle they included a motorsport-grade Inertial Measurement Unit (IMU) (Zeilinger et al., 2017).

The Chinese BIT-FSD team relied mainly on wheel speed sensors to calculate their first driverless vehicle's velocity in 2017. Even though their sensor setup also includes GPS, INS, Lidar and camera sensors, those are separately used to determine the vehicle's position and surroundings. Wheel speed sensors are widely used for odometry calculations in wheeled robots, where the team got this idea from (Tian et al., 2018).

Generally, Bayesian filters provide a statistical tool for dealing with measurement uncertainty, which are described in an easy-to-follow way in (Mochnac et al., 2009). This paper also explains that the probability density function includes all information needed to optimally solve estimation problems in a recursive way, which is why such filter approaches are well suited for velocity estimation. The Extended Kalman Filter is the state-of-the-art estimator for fast, mildly non-linear systems and provides a solution to this problem. The EKF works by linearizing the involved models for every iteration. The GSMS requires the use of an EKF for the attitude estimation.

Noteworthy is also the Doppler-based approach which a French research group from the Sorbonne University Pierre and Marie Curie in Paris elaborately discuss in their paper (Lhomme-Desages et al., 2009). With a low-cost Doppler radar and an accelerometer, the ground speed of a vehicle can also be obtained. The focus of the paper lies on measuring the slip rate, for which an estimation of the true velocity of the vehicle with respect to the ground is necessary. In this paper the authors do not resort to wheel-based methods like optical encoders or resolvers. The Doppler effect principle is as follows: a received electromagnetic wave's frequency is compared to a defined frequency, which changes as the receiver moves with respect to the transmitter. For

their sensor fusion, a simple Kalman filter suffices to fuse the Doppler data and the accelerometer data which outputs an estimate of the longitudinal velocity. With these calculations it is possible to measure the slip rate for each wheel.

### 2.3 System Requirements

The general system requirement regarding a driverless race car is measurement certainty especially while cornering and on wet subsoil. We posed the following additional requirements for the developed system regarding its expandability: The system can be extended to allow further sensors to be added to the sensor fusion without having to reorganise the software structure. The system allows for a simulation of recorded sensor data using tools such as MATLAB. Additional redundancy checks can be programmed to allow for even more precise system outputs. The system can be fully integrated into the future autonomous system of the Formula Student ZHAW driverless car.

### 2.4 Sensor Placement

The sensors may be mounted to the vehicle with a maximum distance of 500 mm above the ground and less than 700 mm forward of the front tires as is depicted in
Figure 1. Furthermore, the vehicle is subjected to a rain test at the races. Therefore, all sensors must be adequately sealed and waterproof.

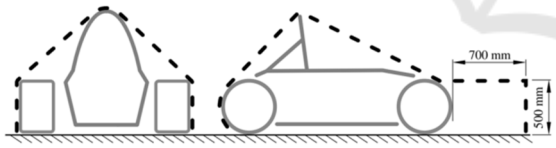


Figure 1: Envelope to mount sensor systems on a formula student race car (FSG 2019).

## 3 SYSTEM CONCEPT AND DESIGN

### 3.1 Overall Concept

The ground speed measuring system is designed to accurately and reliably measure the ground speed of an autonomous vehicle. The system features an Inertial Measurement Unit (IMU) and Global Positioning Sensor (GPS) to measure the ground speed as well as a microcontroller to process the raw sensor readings.

### 3.2 Microcontroller and Sensors

With the sensor fusion of a GPS and an IMU the GSMS can provide an accurate measurement output which is based solely on the two sensors. The IMU measures the following quantities:

- Acceleration (3D): X, Y and Z axes
- Angular velocity (3D): X, Y and Z axes
- Magnetic field strength (3D): X, Y and Z axes

The GPS measures the following quantities:

- Absolute position (3D): Latitude, Longitude, Altitude
- Velocity (3D): Magnitude and angle relative to (true) north, vertical velocity

### 3.3 Sensor Fusion and Data Processing

The measurements from the sensors are processed and combined in a custom sensor fusion algorithm. The custom sensor fusion algorithm consists of multiple stages which perform different filtering and fusion tasks. An overview of the different stages is given in Figure 2. Readings from the implemented sensors must be combined to determine an estimate of the ground speed that is as accurate as possible, for which the GSMS uses two Kalman filters as can be seen in Figure 2. The first Kalman filter is only used to determine the system attitude while the second Kalman filter estimates the final system velocity.

#### 3.3.1 Attitude Kalman Filter

The attitude Kalman filter is an EKF as the equations required to describe the physical properties of the system attitude are non-linear. The attitude Kalman filter is used to track the system attitude, which is represented using a quaternion (the first component of the rotation quaternion describes the angle of rotation and the remaining three components describe the axis of rotation). The attitude of the race car is always described relative to the earth fixed inertial reference frame.

The attitude Kalman filter has a state vector $x$ that tracks the x, y and z components of the attitude error $a$ and the x, y and z components of the gyroscope bias. Therefore, the state vector is a column vector with 6 elements. It is important to note that the attitude Kalman filter does not directly track the quaternion $q_{ref}$ as part of its state vector. Instead, it tracks an attitude error. At the beginning of each iteration, this error is assumed to be zero.

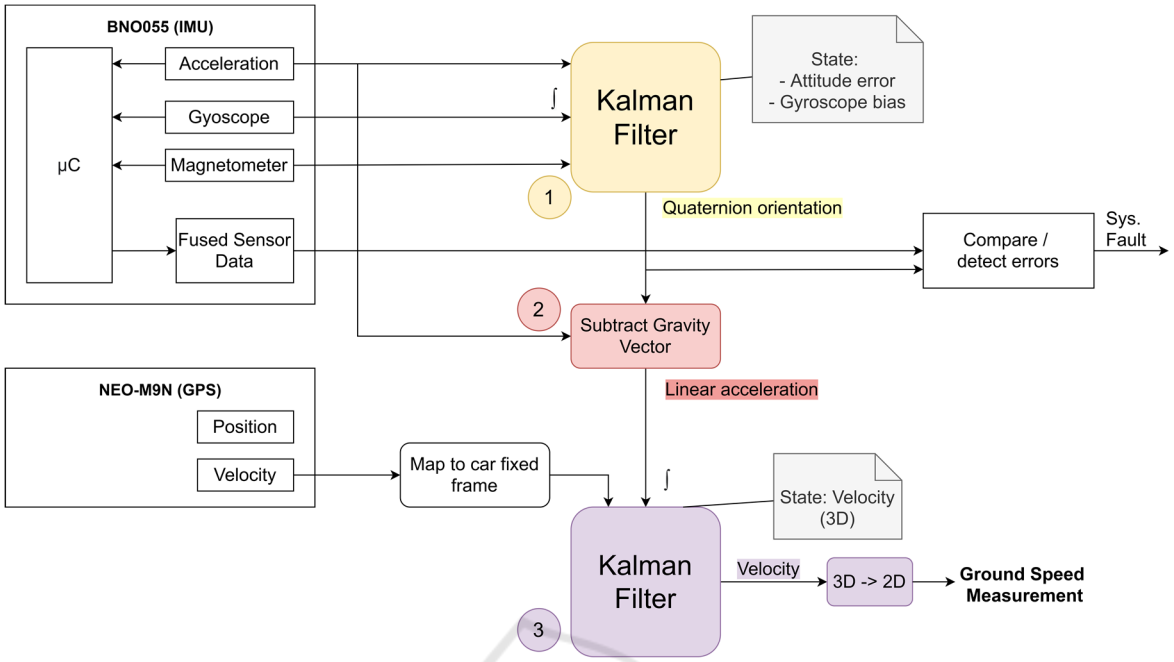


Figure 2: Sensor Fusion Concept.

And at the end of each iteration, the attitude error is added to the reference attitude quaternion $q_{ref}$ and then reset to zero. The system attitude is therefore expressed using two parts as described in the following equation:

$$q(t) = \delta q(a(t)) \oplus q_{ref}(t) \quad (1)$$

The above approach of tracking an attitude error instead of directly tracking the attitude is unique to the attitude Kalman filter. The EKF used to track the attitude in the GSMS therefore is a Multiplicative Extended Kalman Filter (MEKF). The term "multiplicative" refers to the fact that the attitude error $a(t)$ tracked by the attitude Kalman filter is propagated to the reference attitude quaternion $q_{ref}$ using a quaternion multiplication operation. To perform this quaternion multiplication at the end of each iteration, $a(t)$ is first converted into its quaternion representation and then multiplied with $q_{ref}$.

Instead of changing the attitude error $a(t)$, the prediction step directly adjusts the reference quaternion $q_{ref}$. After $q_{ref}$ has been updated, the error covariance matrix $P$ must be updated as well. This is required as the process model introduces new errors. These errors are represented by the process noise covariance matrix $Q$. The steps to update $P$ therefore involve the matrix $Q$. The measurement step of the attitude Kalman filter corrects the previously calculated estimate using absolute measurements of the system attitude. The measurement step is executed twice, as the GSMS uses the gravity vector given by the accelerometer and the North vector given by the magnetometer as two absolute measurements for the system attitude. Finally, the error propagation step must always be called before a new iteration of the attitude Kalman filter algorithm is started.

### 3.3.2 Velocity Kalman Filter

The velocity Kalman filter is a regular Kalman filter as the equations required to describe the system velocity are all linear. This makes the velocity Kalman filter significantly simpler than the attitude Kalman filter. The velocity Kalman filter can also directly track the velocity of the system in its state vector $x$. The state vector $x$ for the velocity Kalman filter contains the x, y and z components of the system velocity.

The initial value for the state vector $x$ is set to the zero vector. The state vector directly tracks the system velocity. Setting the state vector $x$ to the zero vector therefore results in the following initial condition: The system velocity $vel$ is set to the zero vector. The system is usually initialized while the race car is not moving, therefore the above initial value for the system velocity $vel$ is a reasonable choice.

The velocity Kalman filter predicts the system velocity by integrating the linear acceleration measured using the accelerometer. The integral over the linear acceleration $lin\_accel$ is computed using the

time $dt$ that has passed since the last iteration of the algorithm. The GSMS is designed such that $dt$ is always 10ms. After the state vector $x$ has been updated, as for the MEKF, the error covariance matrix $P$ must be updated as well. These errors are represented by the process noise covariance matrix $Q$.

The measurement step of the velocity Kalman filter will correct the previously calculated estimate using an absolute measurement of the system velocity. The GSMS uses the velocity measured in 3 dimensions by the GPS as absolute measurements for the system velocity.

# 4 RESULTS

To test the developed system, we made the following comparisons:

- The output of the custom attitude Kalman filter algorithm was compared to the output of the sensor fusion firmware, which runs on the IMU.
- The output of the custom velocity Kalman filter algorithm was compared to the GPS velocity measurement (which is only available at a lower frequency than the output of the velocity Kalman filter).

## 4.1 Attitude Kalman Filter

The first test was carried out in a residential area by driving around two blocks in a figure of 8. This test was performed at low speeds of around 30 km/h. The goal of this test was to demonstrate that the algorithms of the GSMS are processing the sensor data correctly. The accuracy is only evaluated in a qualitative manner. The performance of the attitude Kalman filter is demonstrated very well using this test. Driving a figure of 8 involved turns in both directions and it ensured that the vehicle was oriented in a variety of different directions throughout the test.

The attitude is represented as a rotation consisting of four components. All attitude plots display the w, x, y and z components of the quaternion separately. Due to the trigonometric functions involved in the quaternion representation of a rotation, the meaning of individual components of a quaternion is often difficult to interpret. Certain individual components displayed in the attitude plots manage to show specific properties of the tests, which will be explained for each plot.

Figure 3 clearly demonstrates that our custom attitude Kalman filter calculates a meaningful system attitude. This claim is supported by the following observations: The graph shows that the x and y components of the plot remain roughly constant around zero. This is the expected behaviour if the vehicle is only rotated around its z axis. The graph also shows that the z component of the quaternion continuously changes its value throughout the test. This is the expected behaviour if the vehicle is driving a figure of 8 on a horizontal plane.

The attitude computed by the custom sensor fusion algorithm can now be compared to the attitude, that is computed by the bno055 sensor fusion firmware. The output of the sensor fusion firmware is displayed in Figure 4.

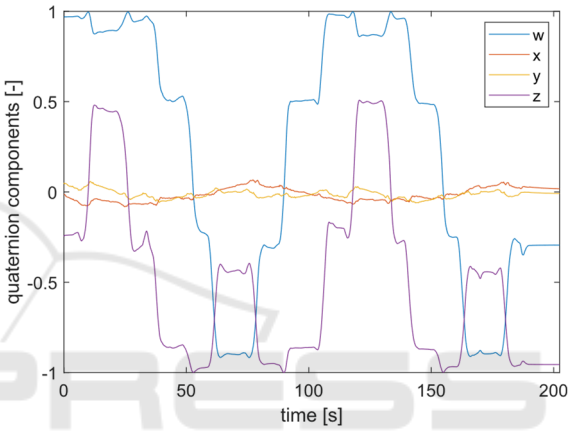


Figure 3: System Attitude (as computed by the custom attitude Kalman filter).

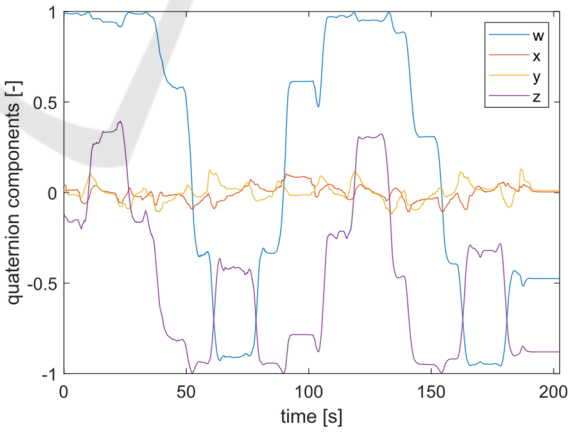


Figure 4: Actual system attitude (as computed by the bno055 firmware).

This graph allows us to prove that the GSMS does not only calculate a meaningful system attitude, but that it is also in line with the output of an independent algorithm. When comparing the two graphs the following can be observed: The custom sensor fusion algorithm implemented in the GSMS com-

putes (qualitatively) the same attitude as the bno055 sensor fusion firmware. The custom sensor fusion algorithm correctly processes the input of all three sensors (accelerometer, gyroscope and magnetometer). The x and y axis of the attitude quaternion measured by our custom sensor fusion algorithm shows higher fluctuation than the output computed by the bno055 sensor fusion firmware. The reason for this is unknown.

Figure 5 shows the angle of the difference in rotation between the attitude computed by the GSMS and by the bno055 sensor fusion firmware. This plot effectively visualizes the difference between the two plots shown before. The plot shows that the difference between the two attitude measurements is usually between 5 and 25 degrees. Our experiments showed that this is mostly caused by magnetic disturbances which influence the measurement made by the magnetometer inside the IMU. The custom sensor fusion firmware starts to output inaccurate attitude values if the magnetometer is not in an ideal environment.

The bno055 sensor fusion firmware on the other hand seems to have a mechanism that detects situations where magnetometer measurements are unreliable. It then most likely stops relying on the magnetometer input until it is able to re-calibrate the magnetometer. The strong magnetic disturbances were mostly caused by the residential area in which this test was performed. The second test was performed in an area with less buildings which lead to an improved performance of the custom attitude Kalman filter.

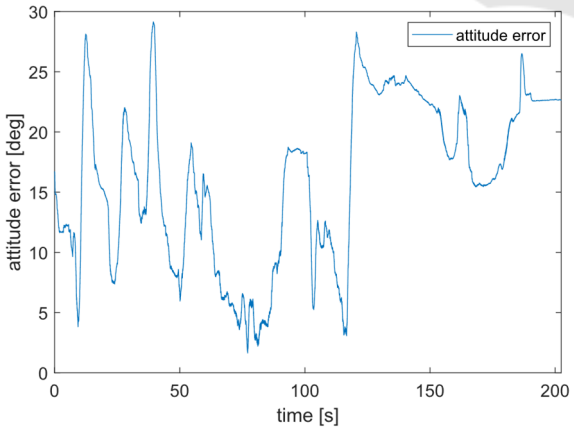


Figure 5: Attitude error.

## 4.2 Velocity Kalman Filter

The test described above is also well suited to demonstrate the performance of the velocity Kalman filter. Figure 6 shows the velocity as it was recorded by the GPS. The plot visualizes all three axes which correspond to the $North(x), East(y)$ and $Up(z)$ axes of the inertial frame. It is important to note that the following plot shows the GPS measurement, which is always made in the inertial frame. The plot shows that the car was moving in different directions on a horizontal plane. Therefore, the GPS measured non-zero values on the x and y axis while the z axis remained constant at zero velocity. This is the expected behaviour.

The plot in Figure 7 shows how the previously calculated system attitude is used to transform the GPS velocity from the inertial frame into the body frame. This plot displays the same velocity as Figure 6 but after it was rotated into the body frame using the system attitude computed by the GSMS. Thus, the plot now shows the three axes x, y and z corresponding to the body frame. We can clearly see that the plot only shows a significant velocity for the y axis. This is the expected behaviour because the y axis is facing in the direction of travel. This is fur

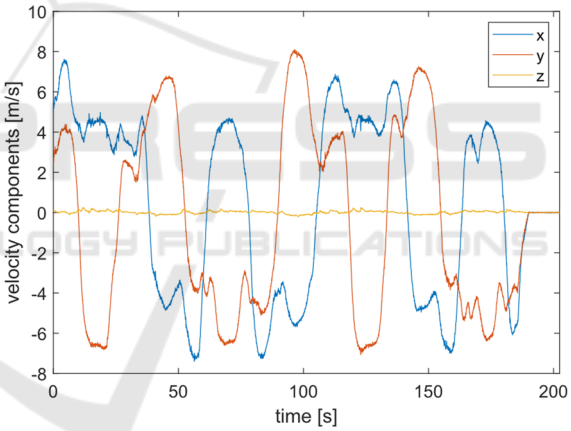


Figure 6: GPS velocity.

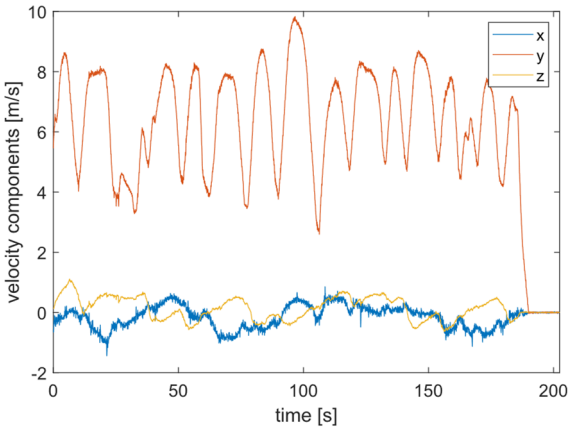


Figure 7: Rotated GPS velocity.

ther proof that the attitude Kalman filter is in fact computing the correct attitude. Because the transformation from Figure 6 to Figure 7 is solely based on this attitude. An incorrect attitude would have caused high non-zero values on the x and z components in Figure 7.

## 4.3 Linear Acceleration

Figure 8 displays the linear acceleration calculated by the GSMS after the gravity vector has been subtracted. Subtracting the gravity vector again involves the previously calculated system attitude.

Figure 9 displays the linear acceleration as it was calculated by the bno055 sensor fusion firmware. These two plots show a similar linear acceleration. Especially high peaks of acceleration are found in both plots. The plots do however not meet the expected behaviour. The expected behaviour would be that both plots continuously show the same values on all three axes. We expect some interference to cause this unexpected behaviour.

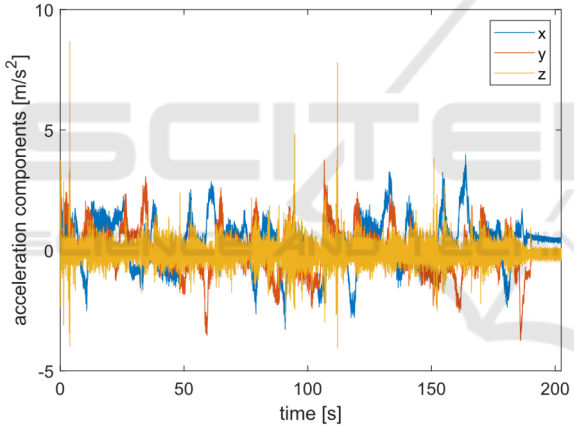


Figure 8: Kalman filter linear acceleration.

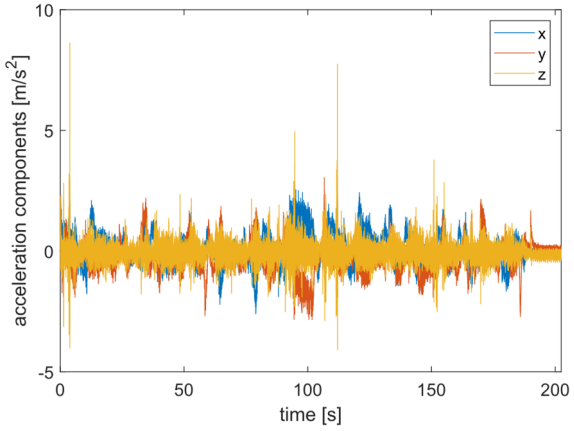


Figure 9: Actual linear acceleration.

## 4.4 Final System Output

This part of the test compares the final output of the custom velocity Kalman filter implemented in the GSMS with the rotated velocity measurement that was recorded by the GPS. Figure 10 visualizes the error between the velocity Kalman filter output and the rotated GPS velocity.

The plot shows two different properties: The angle between the two velocity vectors in degrees (velocity angle error) and the difference in length between the two velocity vectors in m/s (velocity norm error).

The graph can be interpreted as follows: The velocity angle error is usually below 20 degrees and often below 10 degrees. This is the expected behaviour. It proves that the direction of the velocity measured by the GSMS is correct. The velocity norm error is usually below 1 m/s. This is the expected behaviour. It proves that the absolute value of the velocity measured by the GSMS is correct. The velocity angle error increases to values of up to 180 degrees at the very end of the test. This is the expected behaviour for situations where the actual velocity is zero. At the very end of the test, the vehicle was stationary after coming to a halt, and therefore the GSMS as well as the GPS are measuring velocity vectors which are very close to the zero vector. It is expected that the angle between those two vectors can assume any angle in the range of 0 to 180 degrees, as seen in the graph.

Figure 13 shows the final output of the GSMS. This is the signal which will be transmitted to the control unit of the self-driving car. It shows the three components of the vehicle ground speed in the body frame. It clearly shows that the main part of the velocity is measured on the y axis which is facing in the direction of travel. This is the expected behaviour.

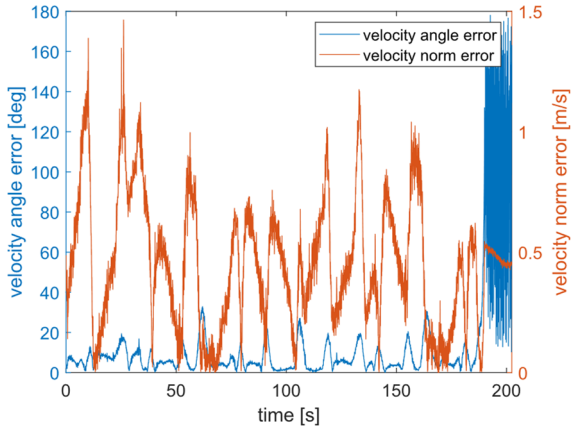


Figure 10: Velocity error.

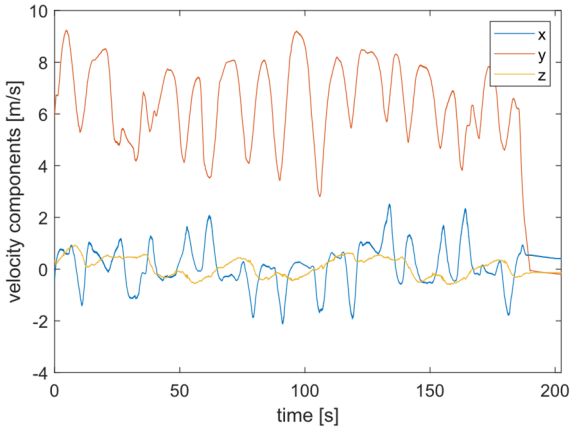


Figure 11: Kalman filter velocity output.

## 5 CONCLUSIONS

One of the main motivations for developing a ground speed measuring system was to take part in the development of an autonomous race car. The idea was to have a reliable and redundant measuring system support the driverless vehicle in various aspects with this sensor fusion output, in order to be eligible to compete with top teams around the world.

In this paper, an approach to a ground speed measuring system using two sensors providing data for sensor fusion was presented. Details were provided on the hardware and software architecture.

The presented ground speed measuring system proved its functionality during testing. The tests performed on the GSMS showed that the custom sensor fusion algorithms are mathematically correct. They produced a qualitatively acceptable and usable output in all tests.

However, the sensor fusion algorithms start to produce inaccurate outputs if the environment does not provide ideal conditions. This could be improved by adding more features to the currently implemented algorithms of the GSMS, such as detection of incorrect sensor measurements (especially for the magnetometer) and/or additional filtering of sensor measurements prior to executing the Kalman filters (specifically a high pass filter for the gyroscope and a low pass filter for the accelerometer when determining the gravity vector).

## REFERENCES

Kabzan, J. et al. (2017). Autonomous Racing Car for Formula Student Driverless. *ROSCon Vancouver 2017*. doi:10.36288/roscon2017-900803

Valls, M. I. et al. (2018). Design of an Autonomous Racecar: Perception, State Estimation and System Integration. *2018 IEEE International Conference on Robotics and Automation (ICRA)*. doi:10.1109/icra.2018.8462829

Zeilinger, M. et al. (2017). Design of an Autonomous Race Car for the Formula Student Driverless (FSD). *Proceedings of the OAGM&ARW Joint Workshop 2017*. doi: 10.3217/978-3-85125-524-9-10

Tian, H., Ni, J., & Hu, J. (2018). Autonomous Driving System Design for Formula Student Driverless Racecar. *2018 IEEE Intelligent Vehicles Symposium (IV)*. doi:10.1109/ivs.2018.8500471

Mochnac, J., Marchevsky, S., & Kocan, P. (2009). Bayesian filtering techniques: Kalman and extended Kalman filter basics. *2009 19th International Conference Radioelektronika*. doi:10.1109/radioelek.2009.5158765

Lhomme-Desages, D., Grand, C., Guinot, J., & Amar, F. B. (2009). Doppler-Based Ground Speed Sensor Fusion and Slip Control for a Wheeled Rover. IEEE/ASME Transactions on Mechatronics, 14(4),484-492. doi:10.1109/tmech.2009.2013713

FSG (2019, September 13). Formula Student Rules 2020. Retrieved February 10, 2021, from https://www.formulastudent.de/fileadmin/user_upload/all/2020/rules/FS-Rules_2020_V1.0.pdf